Asian Pub. Corp.

www.asianpubs.org

ARTICLE

Transition Metal Complexes of *N*-(4-(*N*-(8-Hydroxyquinolin-5-yl)sulfamoyl)phenyl)acetamide ligand: Synthesis, Characterization, *in silico, in vitro* Antimicrobial and DNA Binding Studies

Ruby Kharwar and Ritu B. Dixit✉

Asian Journal of Organic & Medicinal Chemistry

Volume: 5 Year: 2020
Issue: 1 Month: January–March
pp: 20–29
DOI: https://doi.org/10.14233/ajomc.2020.AJOMC-P238

Received: 16 October 2019
Accepted: 14 January 2020
Published: 5 May 2020

ABSTRACT

A new, *N*-(4-(*N*-(8-hydroxyquinolin-5-yl)sulfamoyl)phenyl)acetamide (8HQSPA) ligand and its metal chelates with transition metal salts of Cu(II), Ni(II), Zn(II), Co(II), Fe(II) and Mn(II) was synthesized. The synthesized 8HQSPA ligand was characterized by mass, FT-IR, ^{1}H NMR, ^{13}C NMR and its metal chelates by studying their physico-chemical properties, elemental analysis, FT-IR, thermogravimetric (TG) analysis, UV-visible absorption spectroscopy and magnetic susceptibility. Thermogravimetric analysis result evident presence of two water molecules in the coordination which gives the idea of octahedral geometry and also electronic spectra showed transitions in ligand field and charge transfer bands. *in silico* ADMET studies was carried out to know the biological potential of synthesized compounds as it helps in development of drug candidate with fewer side effects. Molecular docking studies was carried out on bacterial proteins (PDB ID: 5h67, 3ty7, 3t88 and 5i39) and DNA helix (PDB ID: 1BNA) to predict its inhibitory effect and role on integration of DNA helix. Results showed least binding energy score (kcal/mol), which indicate that their potential of binding is greater in receptor of proteins and binds DNA through intercalation mode, which was further assessed by *in vitro* experiments. Antibacterial studies were carried out in the form of minimum inhibitory concentration (MIC), the results showed increased biological activity of free ligand on metal complexation in the following order: Cu > Fe > Zn > Ni > Co > Mn > 8HQSPA. Also interaction of complexes with CT-DNA was carried out by viscosity measurement, electronic absorption titration and gel electrophoresis, showed intercalation mode of binding.

KEYWORDS

Sulfonamide, 8-Hydroxyquinoline, Antibacterial, DNA binding, ADMET, Molecular docking.

Author affiliations:

Ashok and Rita Patel Institute of Integrated Study and Research in Biotechnology and Allied Sciences (ARIBAS), New Vallabh Vidyanagar-388121, India

✉To whom correspondence to be addressed:

E-mail: ritsdixit@yahoo.co.in

Available online at: http://ajomc.asianpubs.org

INTRODUCTION

A rapid increase in the development of microbial resistance from existed drugs leads urgent need to develop antimicrobial agents with improved efficacy, lower side effect and less toxic [1,2]. Molecular hybridization based drug design approach has been exploited over the years by many researchers to develop some promising new hybrid chemical entities showing significant therapeutic values. Combining two pharmacophores into a single molecular skeleton is a well established approach in

designing more potent drugs with a significant increased activity. Rather than using drugs in combination, a hybrid molecule acting on manifold targets considers to be a better drug candidate since administration of single drug will have more predictable pharmacokinetic and pharmacodynamic properties with improved patient compliance.

Heterocyclic compounds remain the first choice ever to design a newer class of structural entities of medicinal importance [3]. 8-Hydroxyquinoline (8HQ) is considered as a privilege structure to design a new drug compound because of its vast applications as antibacterial, antifungal, antiamoebic, anticancer, antiviral and antineoplastic agents [4-6]. To design new drug candidate, 8-hydroxyquinoline and its derivatives are extensively used as a ligand in coordination chemistry as its planer heterocyclic scaffold has N and O donor atom and serves as a bidentate chelator for metal ions [7]. The mode of action of 8HQ as antibacterial and anticancer agent has been studied and it is due to the metal complexation of 8HQ [8]. Also interaction with metal ion is required for antiproliferative activity, as to inhibit the cancer cell growth, the binding with copper ion and its transportation into cells are must [9].

Sulfonamides and its derivatives holds a prominent position in medicinal chemistry research due to its wide application as pharmaceutical agents but various bacterial strains have developed resistance against them [10,11]. Sulfonamide groups are now added to biologically active scaffolds to generate new effects. For example, potent inhibitors of Alziheimer disease associated with butyryl cholinestarase have been developed by synthesizing sulfonamide analogs of earlier hit compounds which showed *in vivo* activity in low concentrations [12] and this is how the use of sulfa drugs has been extended in treating more complex diseases such as Alziheimer disease, central nervous system disorders, various cancers and tumors, diabetes, leprosy, psychosis, malaria and tuberculosis. And also, since the discovery of sulphanilamide, researchers are making efforts to synthesize newer sulfonamide (-SO_2NH-) derivatives [13].

Metal plays an important role in various biological processes. They exert their effect by coordinating to oxygen and nitrogen terminals of proteins in variety of models and play a decisive role in the conformation and function of biological macromolecules [14]. Since the landmark discovery of cisplatin, metallodrugs have been a subject of interest. Recent research proves that the activity of many drugs have been increased upon metal complexation and have been extensively studied to identify their potentials as anticancer drugs by studying its DNA disentangle efficiency [15]. This study also renders pathways for the development of new antimicrobial agents.

Additionally *in silico* drug designing is a way to predict more than one thousand biological and toxicological activities simultaneously by using structural formula of the organic compounds [16,17]. This helps in generating lead compound more accurately.

This study was carried out with an aim to synthesize a new 8-hydroxyquinoline-sulfonamide hybrid chemical entity (ligand) and its metal chelates. *in silico* ADMET (adsorption, distribution, metabolism, excretion and toxicity) and biological activity prediction of synthesized compounds and DNA binding analysis are also studied. *in vitro* antibacterial activity was carried out to study their synergistic effect as a ligand and the role of metal complexation on bacterial growth. DNA binding study was also carried out which further felicitates the understanding of cell growth inhibition.

EXPERIMENTAL

The experimental protocol and dealing of instrumental techniques of UV-visible absorption method, antimicrobial activity, *in silico* ADMET properties and molecular docking studies are given in the supporting information file. DNA interaction studies by means of UV-visible absorption titration, viscosity measurement and agarose gel electrophoresis is also described thoroughly in the supporting information file.

The reaction and purity of the compounds was monitored by ascending thin layer chromatography (TLC) on silica gel F254 thin-layer chromatographic plates of size 20 × 20 cm was purchased from the Merck (India) Limited. Melting points were checked by the open capillary method and are uncorrected. The elemental analysis was performed with C, H, N, S analyzer on Perkin Elmer (U.S.A, 2400 Series II). The infrared spectra (FT-IR) were obtained from KBr pellets in the range 4000-400 cm^{-1} with a Perkin Elmer spectrum GX spectrophotometer (FT–IR) instrument. The mass (ESI-MS) spectrum of *N*-(4-(*N*-(8-hydroxyquinolin-5-yl)sulfamoyl)phenyl)acetamide (8HQSPA) was recorded on a Shimadzu LC-MS 2010 eV mass spectrophotometer in methanol. ^{1}H NMR and ^{13}C NMR was recorded on a Bruker (400 MHz) instrument using DMSO-d_6 as solvent as well as an internal reference standard. Thermogravimetric analyses were carried out with a model Perkin-Elmer Thermogravimetry analyzer at a heating rate of 10 °C min^{-1} in air. The metal contents of the complexes were examined by EDTA titration after decomposing the organic matter in mixing $HClO_4$, H_2SO_4 and HNO_3 (1:1.5:2.5).

Synthesis of 4-acetamidobenzenesulfonyl chloride has been done according to reported method [18]. The synthesis of *N*-(4-(*N*-(8-hydroxyquinolin-5-yl)sulfamoyl)phenyl)acetamide (8HQSPA) has been done by modification of the reported method in convenient manner [19]. The outline of the synthesis of 8HQSPA and its M(II) chelates is shown in **Scheme-I** and the physiochemical parameters of 8HQSPA and metal(II) complexes are summarized in Table-1.

Synthesis of *N*-(4-(*N*-(8-hydroxyquinolin-5-yl)sulfamoyl)phenyl)acetamide (8HQSPA): 4-Acetamidobenzenesulfonyl chloride (0.75 mmol) was added drop wise to 5-amino-8-hydroxyquinoline dihydrochloride (0.70 mmol) in dry pyridine at 0 °C. The solution was stirred for 6 h at 0 °C while, reaction was monitor by TLC. The excess of pyridine was distilled off and the residue was quenched into ice-cold water to get green solid product which was collected by filtration, washed with ethyl acetate, chloroform and dried *in vacuo* [19]. ESI-MS: 355.75 (M+1) *m/z*. ^{1}H NMR (400 MHz, DMSO-d_6, δ_H, ppm) of 8HQSPA is assigned as follows: 10.032 (s, 1H), 9.065 (s, 1H), 8.9985 (d, 1H), 7.979 (s, 1H, 7.589 (d, 3H) 7.398 (d, 1H), 7.277 (m, 3H), 7.014 (s, 1H) 2.044 (s, 3H). ^{13}C NMR (DMSO-d_6) (δ): (aromatic, C) obtained at 113.55, 115.65, 118.92, 121.92, 122.87, 124.42, 128.58, 129.05, 133.20, 135.92, 139.34, 142.64 and 148.02 ppm, peak at 23.95 ppm belongs to (–CH_3) and 168.24 ppm belongs (–N-CHO).

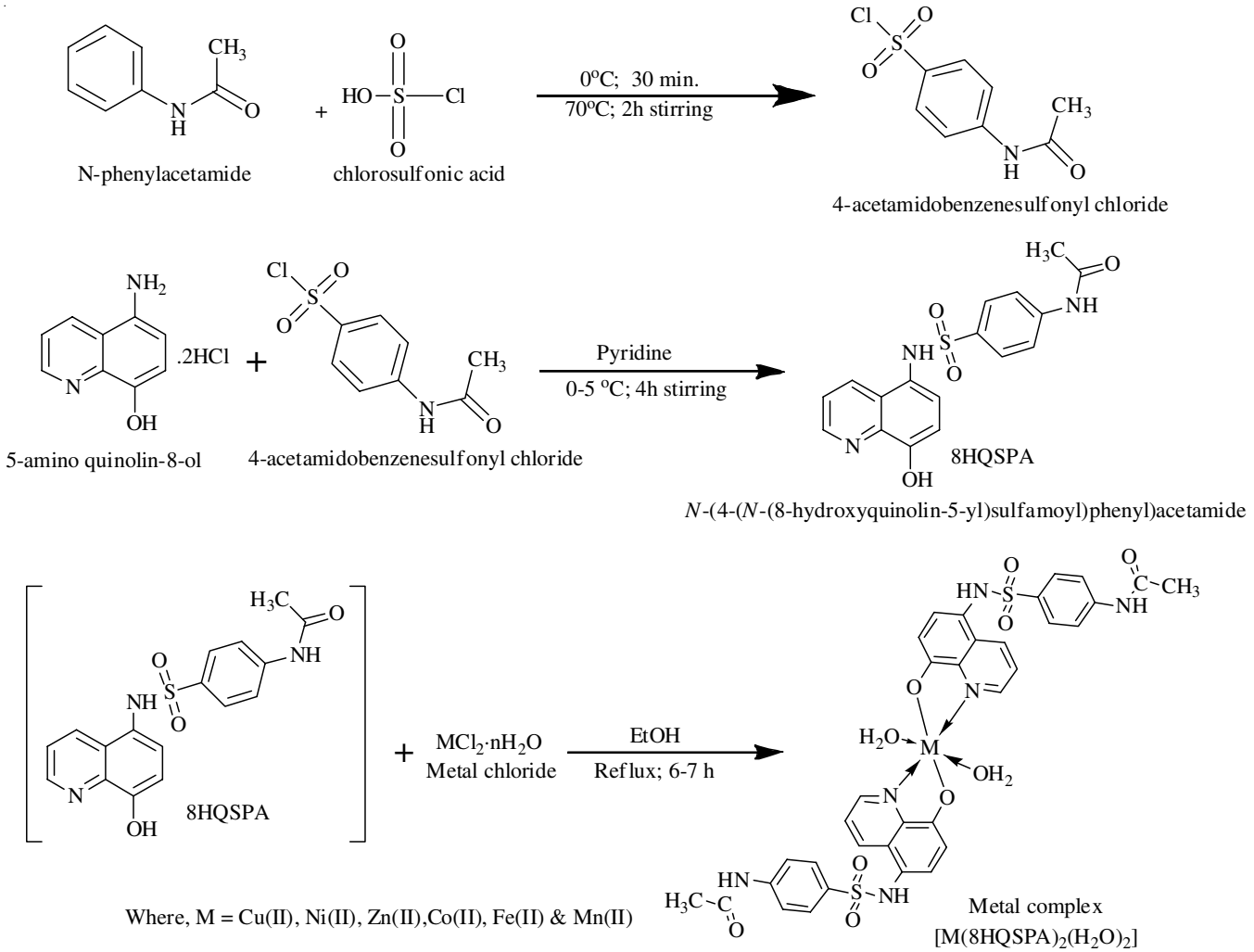

Scheme-I: Proposed route for the synthesis of *N*-(4-(*N*-(8-hydroxyquinolin-5-yl)sulfamoyl)phenyl)acetamide (8HQSPA) and its metal chelates

TABLE-1
PHYSIOCHEMICAL PROPERTIES OF LIGAND AND METAL COMPLEXES

Compd.	m.w.	Colour	Yield (%)	m.p. (°C)	Elemental analysis (%): Found (calcd.)					μ_{eff} (B.M.)
					C	H	N	S	M	
8HQMBS	357.38	Dark green	60	>180	57.02 (57.13)	4.12 (4.23)	11.70 (11.76)	8.85 (8.97)	–	–
8HQMBS-Ni	771.45	Greenish yellow	78.94	>220	52.89 (52.94)	3.55 (3.66)	10.78 (10.89)	8.25 (8.31)	7.59 (7.61)	2.25 (2.38)
8HQMBS-Cu	776.3	Green	90.25	>250	52.55 (52.61)	3.57 (3.64)	10.85 (10.83)	8.28 (8.26)	8.02 (8.19)	1.68 (1.73)
8HQMBS-Fe	768.6	Black	89.22	>250	53.17 (53.13)	3.59 (3.67)	10.85 (10.93)	8.27 (8.34)	7.19 (7.29)	4.88 (4.9)
8HQMBS-Co	771.69	Light green	85.56	>250	52.91 (52.92)	3.68 (3.66)	10.78 (10.89)	8.28 (8.31)	7.58 (7.64)	3.72 (3.87)
8HQMBS-Mn	767.69	Brownish	84.45	>250	53.14 (53.2)	3.59 (3.68)	10.88 (10.95)	8.26 (8.35)	7.11 (7.16)	5.85 (5.92)
8HQMBS-Zn	778.13	Yellow	82.62	>250	52.36 (52.48)	3.55 (3.63)	10.69 (10.8)	8.17 (8.24)	8.28 (8.4)	D

Synthesis of metal(II) complexes of 8HQSPA: M(II)-(8HQSPA)$_2$; M = Cu(II), Ni(II), Zn(II), Co(II), Fe(II) and Mn(II): The synthesized ligand 8HQSPA (0.02 mol) was dissolved in ethanol and the reflux temperature was maintained. To this, warm solution of corresponding metal(II) chloride (0.01 mol) was added drop wise maintaining pH (~8.5) with 10 % NaOH. The mixture was allowed to reflux for 6-7 h on water bath till solvent reduces to smaller volume and centrifuged. The suspended solid formed was collected, filtered and washed with hot distilled water, acetonitrile and dried in vacuum desiccators over calcium chloride [20]. The resultant yield was calculated and the results of elemental analysis of the prepared chelates are represented in Table-1.

RESULTS AND DISCUSSION

The results of elemental analysis (C, H, N and S) are given in Table-1, which shows that they are in concordance with their predicted molecular formula of ligand and its metal(II) chelates and also confirms 2:1 stoichiometery ratio of ligand and metals in the structure.

Mass spectrometry: The formation of ligand 8HQSPA has been studied with ESI-MS in methanol solution. The mass spectra of ligand shows a prominent peak at *m/z* = 355.75 corresponds to $[C_{17}H_{15}N_3O_4S]^-$ and are in good agreement with formula weight of the proposed structural formula $C_{17}H_{15}N_3O_4S$ of 8HQSPA ligand.

FT-IR spectra of 8HQSPA and its metal chelates: The band observed between 1180-1140 cm^{-1} in all the synthesized compounds belongs to $–SO_2NH$, which signifies the structure of ligand. The (C-O) stretching of free –OH molecule at 1080.55 cm^{-1} is shifted to higher frequencies in the spectra of metal chelates. Also the stretching of free –OH at 1322 cm^{-1} in the spectra of ligand 8HQSPA has shifted to higher frequencies in all the metal complexes with a strong absorption bands at 1359, 1374, 1380, 1385, 1380 and 1379 cm^{-1} for Mn(II), Zn(II), Cu(II), Ni(II), Co(II) and Fe(II) metal chelates, respectively indicates the coordination of 8-hydroxyquinoline in the metal complexes. The significant difference to be expected in the IR band of 8HQSPA and its metal chelates was the presence of more broadened band in the region of 3500-2800 cm^{-1} of free –OH which form coordination bond with the metal ions and also explains the presence of coordinated water molecule. The other expected difference was the band due to C–N stretching of 8-hydroxyquinoline at around 1650 cm^{-1} in the IR spectrum of 8HQSPA was shifted to a lower frequency. This was further confirmed by a weak band around 1220 cm^{-1} corresponding to C–O–M stretching after deprotonation, while bands exhibited within the range of 550 and 415 cm^{-1} correspond to M–O and M–N vibration, respectively [21,22].

^{1}H and ^{13}C NMR spectroscopy: The formation of ligand 8HQSPA was further confirmed by ^{1}H and ^{13}C NMR spectra in DMSO-d_6 solution using TMS as a standard represented. It can be seen that the spectra of ligand shows a singlet peak at δ 10.032 integrates for aromatic –N*H*Ac and broad singlet peak appeared at δ 9.065 is of –O*H* merged with $–SO_2N$*H*. 8.9985 (d, *J* = 6.8Hz, 1H, $–SO_2N$*H*–, Merged with O*H*), the peak at δ 7.979 belongs to Ar*H*, in pyridine ring next to –N and doublet peak at δ 7.589 belongs to hydrogen of benzene ring next to Sulphonamide. The hydrogen of pyridine ring is observed on peak δ 7.398 and peak at δ 7.277 belongs to aromatic 2H of benzene ring of sulphonamide next to –N*H*–, 1H of pyridine ring at C3 Proton. The peak observed at δ 7.014 is of aromatic hydrogen in benzenoide ring next to –O*H* and δ 2.044 is of 3H of Ar–NHCOCH_3.

^{13}C NMR spectra represented in concordance with the proposed structure. In the ^{13}C NMR spectrum of 8HQSPA, all the aromatic carbon peaks were observed on δ 113.55, 115.65, 118.92, 121.92, 122.87, 124.42, 128.58, 129.05, 133.20, 135.92, 139.34, 142.64, 148.02 ppm, at δ 168.24 ppm of Ar–NHCO and at 23.95 ppm of carbon in CH_3 group.

Electronic spectra and magnetic moment: An electronic spectrum gives the information about the electronic structure of synthesized ligand and its metal complexes. The UV-visible absorption spectra of 3 mmol DMSO solutions of 8HQSPA ligand and its metal chelates were recorded and are represented in Table-2. The absorption spectrum of ligand 8HQSPA shows two peaks at λ_{max} = 246.46 nm and λ_{max} = 317.74 nm is due to π→π* transition of the conjugated ligands, where as the absorption peak at λ_{max} = 389.01 nm can be assigned to n→π* transition of conjugated quinoline rings [23,24]. But a remarkable difference is noticed in the absorption spectra of its metal chelates (Fig. 1). From the spectra of metal chelates it is seen that the main absorption peak is shifted towards the right side (red shift) between 310-330 nm which suggests ligand centered π→π*

TABLE-2
UV-VISIBLE ABSORPTION TITRATION DATA

Compound	λ (nm)	Absorbance	Transition	ε_{max}	Suggested structure
L	246.46	0.95	π→π*	82,000	–
	317.34	0.09	n→π*	105,780	
	389.01	0.05	n→π*	129,67	
Cu	247.21	0.88	π→π*	82,403	Distorted Octahedral
	320.20	0.36	Ligand field	106,733	
	472.76	0.12	L→M	157,587	
Ni	246.25	0.90	π→π*	82,083	Distorted Octahedral
	315.00	0.34	Ligand field	105,00	
	469.91	0.19	$^3A_2g \rightarrow {}^3T_1g$	156,637	
Zn	249.74	0.60	π→π*	82,083	Octahedral
	329.82	0.11	Ligand field	109,940	
	396.08	0.10	M→L	132,027	
Co	246.54	0.82	π→π*	82,247	Distorted Octahedral
	325.50	0.12	Ligand field	108,500	
	406.34	0.06	$^4T_1g \rightarrow {}^4A_2g$	135,447	
Mn	246.11	0.82	π→π*	82,037	Octahedral
	320.50	0.58	Ligand field	106,833	
	413.89	0.10	L→M	137,963	
Fe	246.11	0.76	π→π*	82,037	Octahedral
	310.40	0.12	Ligand field	103,467	
	473.92	0.10	$^5T_2g \rightarrow {}^5Eg(D)$	157,973	

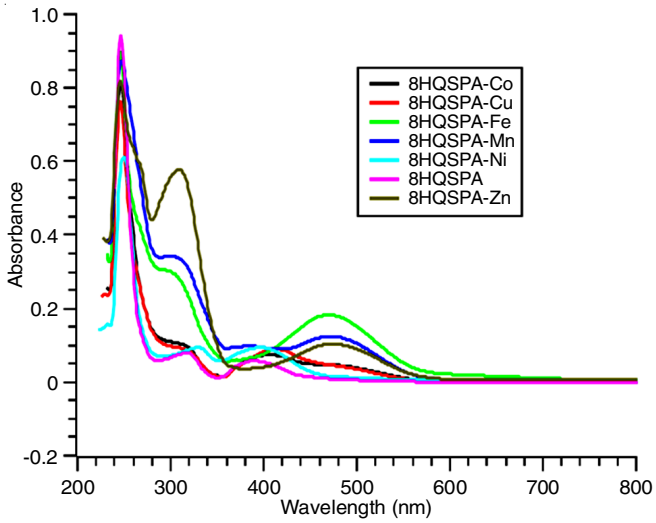

Fig. 1. Absorption titration spectra of ligand 8HQSPA and its metal complexes

transition. The emerging absorbance in the visible range around 396.08 nm in the spectra of Zn(II) is due to the absence of *d-d* transition and can be attributed to metal-to-ligand charge-transfer transitions (MLCT). These values are in concordance with octahedral geometry of the complex [25]. A noticeable hypochromic shift of ligand band is also observed between 310 to 330 nm of Mn(II), Co(II), Ni(II) and Fe(II) complexes is attributed to $\pi \rightarrow \pi^*$ transition of the conjugated ligands of the metal chelates. The bathchromic shifts obtained to higher side at 473.92, 406.34, 469.91 and 413.89 nm in Mn(II), Co(II), Ni(II) and Fe(II) metal chelates belongs to M→L charge transfer and shows the formation of octahedral geometry of the complexes. These kinds of results are the main characteristic of 8-hydroxyquinoline containing complexes in which the complexation is accompanied by deprotonation of the phenolic group [26]. The absorption peak at λ_{max} = 365.5 nm in Cu(II) complex can be attributed to $\pi \rightarrow \pi^*$ transition of conjugated ligands and λ_{max} = 472.76 nm can be due to M→L charge transfer and these results are in concordance with distorted octahedral geometry of the complex [27]. The magnetic moment value obtained at 5.90, 2.92 and 4.61 B.M. at room temperature is typical for distorted octahedral chelates for Mn(II), Ni(II) and Fe(II) complex, respectively [28]. The value obtained of Cu(II) chelates effective magnetic moments 1.85 B.M. is typical for distorted octahedral geometry and the Co(II) complex has magnetic moments values 4.02 B.M. which agreed with the expected value for a high spin Co(II) ion in octahedral environment [29]. The Zn(II) complex is diamagnetic [30].

TGA: Thermogravimetric analysis (TGA) of a compound helps to understand its thermal stability. It also helps to ascertain the nature of associated water molecule and its compositional differences. TG analysis was carried out for the synthesized ligand (8HQSPA) and its metal chelates in the temperature range, 50 to 650 °C in air at a heating rate of 10 °C per min. The TG curves of Cu(II), Zn(II), Ni(II), Mn(II), Fe(II) and Co(II) metal chelates of 8HQSPA has shown two step decomposition pattern, one in the range of 50-150 °C and other in 150-650 °C. The first step decomposition in the range of 50-150 °C is due to the loss of coordinated water molecules in Cu(II) and Ni(II) chelates (Figs. 2 and 3). The second mass loss curve within the temperature range 150-600 °C is due to the decomposition of ligand molecules of Cu(II), Zn(II), Ni(II), Mn(II), Fe(II) and Co(II) complexes. And the remaining residual mass is attributed to left over metal oxides. On the other hand, a thermogram of 8HQSPA (Fig. 4) shows one-step decomposition pattern in the temperature range of 180-250 °C, which gives us insight about its melting point. Thus TG analysis confirmed the octahedral geometrical arrangement of synthesized Cu(II), Zn(II), Ni(II), Mn(II), Fe(II) and Co(II) metal complexes of 8HQSPA [31].

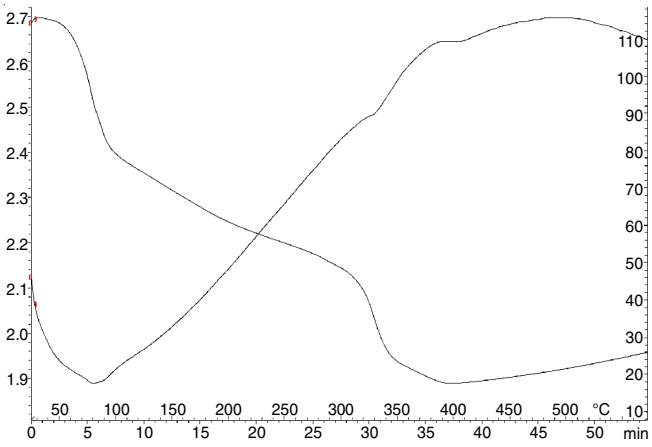

Fig. 2. Thermogravimetric curve of 8HQSPA-Cu(II) metal complex

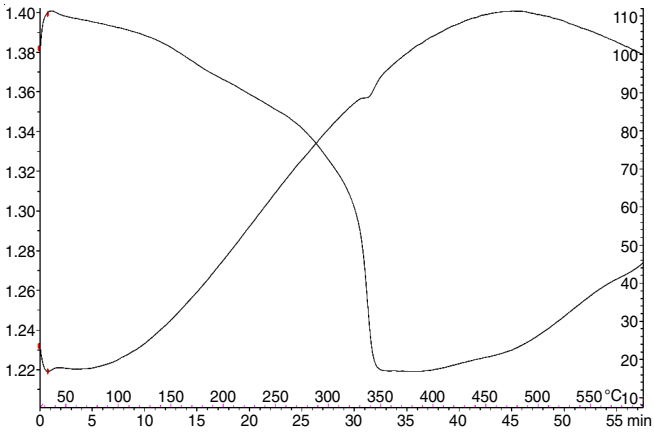

Fig. 3. Thermogravimetric curve of 8HQSPA-Ni(II) metal complex

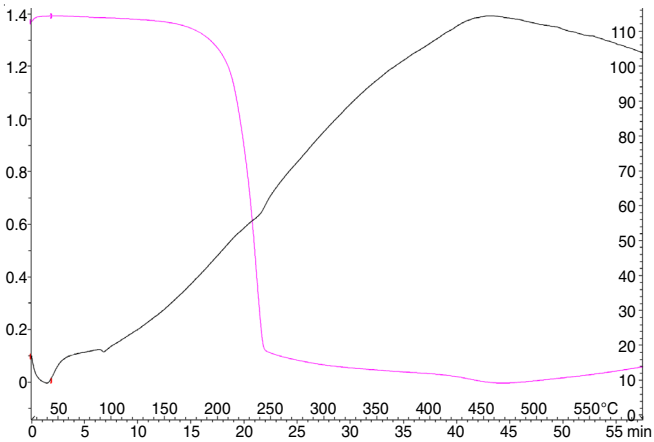

Fig. 4. Thermogravimetric curve of ligand 8HQSPA

***in silico* analysis**

ADMET properties prediction by online *Pre* ADMET tool: *in silico* ADMET (adsorption, distribution, metabolism, excretion and toxicity) properties of all the synthesized compounds has been screened by free online tool, *Pre* ADMET predictor. The pharmacokinetics behaviour of the synthesized compounds has been summarized in Table-3.

The synthesized compound must follow Lipinski rule of five to be considered as a drug candidate. Lipinski rules says that log P value must be less than or equal to five, which is measurement of a compound's tendency to penetrate into the biological membrane. The log P values of synthesized compounds obtained are within permissible range. TPSA (tropical polar surface area) parameter study helps to predict the transportation of drugs inside the various parts of the body like gastro intestinal tract, blood brain barrier (BBB), cell membrane and also its oral bioavailability. The TPSA values [32] are below 140° of studied compounds, which suggests their efficient transport inside the intestine and good bioavailability [33].

The number of hydrogen bond donor and number of hydrogen bond acceptor must be ≤ 5 and ≤ 10, respectively which gives the idea of absorption of compound. The values of tested compounds are represented in Table-3, show strong absorption and hence reveals that they are active in oral mode of administration. Also the drug likeness score are greater than zero, which supports their non-toxicity character. This study reveals that all the synthesized compounds fulfil the criteria of Lipinski rule to be considered as a drug compound.

***in silico* antibacterial studies:** *in silico* antibacterial studies were carried out on proteins of microorganism's such as *Escherichia coli* (PDB ID: 3t88), *Staphylococcus aureus* (PDB ID: 3ty7), *Bacillus subtilis* (PDB ID: 5h67) and *Proteus vulgaris* (PDB ID: 5i39) in order to confirm *in vitro* studies [34]. The results are compared with standard drug sulfamethoxazole and are summarized in terms of binding energy (kcal/mol) (Table-4). The lower binding energy values evident binding of a compound strongly to a protein receptor. The binding energy of synthesized compounds is less than that of sulfamethoxazole, which signifies its good potency as antibacterial drugs. 2D image of Fe(II) complex interacted with protein of *Escherichia coli* (PDB ID: 3t88) is shown in Fig. 5. The results were in concordance with *in vitro* studies wherein the metal chelates are binding strongly than ligand 8HQSPA [34].

Molecular docking: Molecular docking is one of the rational drug design and biological systematic technique, which is used to define the type of interaction, inhibitor potential or the mechanism of chemical entity in receptor. The molecular docking study of synthesized compounds was carried out with B-DNA (PDB ID: 1BNA) using AutoDock 4.2 tools [35] and

TABLE-3
EVALUATION OF IN SILICO ADMET PARAMETERS OF SYNTHESIZED COMPOUNDS

Compounds	log P	TPSA	Number of H-bond acceptors	Number of H-bond donor	Drug likeness score
8HQSPA	1.633	116.77	7	3	0.807
8HQSPA-Zn	1.520	121.75	9	3	0.880
8HQSPA-Cu	1.860	125.25	9	3	0.880
8HQSPA-Fe	2.120	126.23	9	3	0.880
8HQSPA-Co	0.895	121.09	9	3	0.880
8HQSPA-Mn	3.206	122.05	9	3	0.880
8HQSPA-Ni	0.845	121.50	9	3	0.880

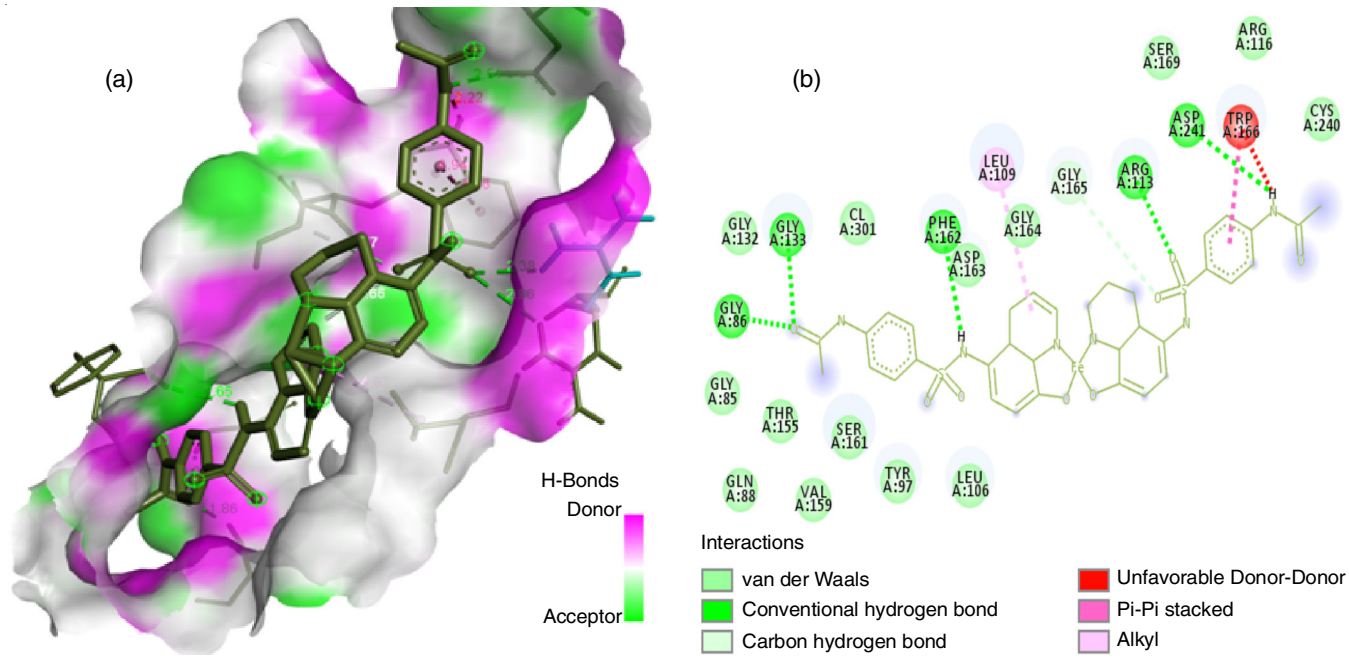

Fig. 5. 3D and 2D image of Fe(II) complex docked with bacterial protein (PDB:ID 3t88)

TABLE-4
in silico MOLECULAR DOCKING STUDIES OF LIGAND AND METAL CHELATES WITH BACTERIAL PROTEINS IN TERMS OF BINDING AFFINITY (kcal/mol)

	Name	8HQSPA	8HQSPA-Co	8HQSPA-Fe	8HQSPA-Mn	8HQSPA-Ni	8HQSPA-Zn	8HQSPA-Cu	Sulfamethoxazole
PDB: ID	5h67	-8.2	-9.5	-9.5	-10.5	-10.2	-11.5	-9.8	-6.2
	3ty7	-8.6	-9.9	-11	-10.6	-10.5	-12.2	-9.2	-6.5
	3t88	-8.6	-9.1	-10.2	-10.9	-10.1	-11.6	-9.5	-6.1
	5i39	-8.4	-9.5	-9.9	-10.5	-10.2	-11.5	-9.6	-6.0

the results were visualized using PyMol and Discovery Studio Visualizer. The result showed that the compounds interact with DNA helix by means of intercalation mode with -11.2 kcal/mol binding affinity. Binding energy score tells us about the binding ability of the compound onto the receptor.

in vitro analysis

Antimicrobial study: For the antimicrobial studied the stock solution of metal complexes and ligand was prepared in distilled DMSO in the concentration of 100 mg/mL. The antimicrobial activity was performed against two Gram-positive (*Staphylococus aureus* and *Bacillus subtilis*) and two Gram-negative (*Pseudomonas aeruginosa* and *Escherichia coli*) strains of bacteria. These strains have developed resistance against many drugs through biochemical and morphological modifications. Here an attempt has been made to study the antimicrobial effects of ligand and its metal chelates and its mode of action. Antibacterial activity was determined as minimum inhibitory concentration (MIC) by micro dilution method given by Clinical Laboratory Standards Institute (CLSI) in comparison to standard drug gatifloxacine, its parent moiety 8-hydroxyquinoline and sulphanilamide [13,14]. The bacterial culture was inoculated in 50 mL autoclaved Muller Hilton Broth incubated at 37 °C on 200 rpm for 24 h. these overnight grown bacterial strains OD was adjusted and then further inoculated at 10 % of MH broth containing antibiotics in concentration gradient 0.1 to 10 µg/mL (arithmetic progression) followed by incubation at 37 °C for 24 h. A positive control with no antibiotic was also prepared and treated similarly. Negative control (uninoculated broth) was subtracted from test readings (OD) taken at 620 nm [15,16]. MIC was considered as test reading when at par with negative control. The results in the form of minimum inhibitory concentration (MIC) are summarized in Table-5.

The results in the form of minimum inhibitory concentration (MIC) are summarized in Table-5. Bactericidal effect of a compound under investigation dependent upon ligands property, lipophilicity, nature of metal ion, its coordination state and geometry of the complex. From the result it is clearly visible that 8HQSPA has better effect on Gram-positive bacteria than that of Gram-negative bacteria because the metal chelating property of 8HQSPA helps its transportation inside the cell membrane of bacteria whereas its activity is less in Gram-negative due to the selective barrier membrane of Gram-negative bacteria. Similar pattern of bactericidal activity is visible for metal chelates also. But a noticeable difference is that the metal chelates are showing batter activity than that of ligand 8HQSPA. This is due to increase in the lipophilicity of coordinated compounds because of its geometrical arrangement which increases their affinity to penetrate inside the cell wall and exerts its activity through oxidation stress or by inhibiting the enzyme metal binding site and blocking its activity [36].

DNA binding studies

DNA binding study through hydrodynamic measurement (viscosity measurement): Viscosity experiment was carried out using Ubbelohde viscometer and a constant temperature (37 °C ± 1) was maintained using thermometric bath. Each sample run was measures three times with the help of digital stop, watch and the average flow time was calculated to assess the viscosity (η) of the samples. The concentration of CT DNA was fixed at 200 µM in phosphate buffer (Na_2HPO_4/NaH_2PO_4, pH 7.2). The relative specific viscosity were represented as $(\eta/\eta_0)^{1/3}$ *vs.* binding ratio (r) of [DNA]/[complex] = 0.0, 0.04, 0.08, 0.12, 0.16, 0.20 µM, where η is the relative viscosity in the presence of complex and η_0 is the relative viscosity of DNA alone.

DNA binding study through UV-visible spectrophotometer: Probing metal-DNA interaction can be done easily by UV-visible electronic absorption titration as the spectrum gets perturbed on interaction with each other. DNA binding experiment was recorded using double beam spectrophotometer. The results were studied in the presence of CT DNA (Calf Thymus DNA) at a constant concentration of the 8HQSPA and its metal

TABLE-5
ANTIMICROBIAL ACTIVITY OF 8HQSPA AND ITS Cu(II), Zn(II), Ni(II), Mn(II), Fe(II) AND Co(II) METAL CHELATES

Compounds	Minimum inhibitory concentration MIC (µg/mL)			
	S. aureus	*B. subtilis*	*E. coli*	*P. aeruginosa*
8HQSPA	4.0	4.0	10.0	9.0
8HQSPA-Zn	3.25	3.5	8.0	7.5
8HQSPA-Cu	3.25	3.0	7.5	6.5
8HQSPA-Fe	3.5	3.25	7.5	7.0
8HQSPA-Co	4.0	4.25	8.5	7.5
8HQSPA-Mn	4.75	4.50	9.0	6.5
8HQSPA-Ni	3.5	4.0	8.75	7.25
8HQ	6.0	6.0	> 20	> 20
Sulphanelamide-sulphate	NT	NT	NT	NT

oxinates (10 µM) dissolved in DMSO and phosphate buffer (pH 7.2). The volume of DMSO was kept below 1 % v/v in order to prevent denaturation of DNA under investigation. The results were recorded by taking 10 µL of 8HQSPA/metal coxinates and CT DNA in phosphate buffer [19] with pH 7.2.

DNA binding study through gel electrophoresis: The ligand/complex-DNA interaction was also carried out by gel electrophoresis by measuring the retarded motion of CT DNA in the agarose gel on interaction with the ligand/complex. DNA sample was taken in the concentration of 1.4×10^{-5} M and were determined spectrophotometrically by employing an extinction coefficient of 6600 M^{-1} cm^{-1} at 260 nm. The 8HQSPA/metal complex concentration was also fixed at 1.6×10^{-5} M. Incubation times (2 h) was allowed upon addition of complexes in DNA solution. 8 % agarose gel was prepared and 10 µL of sample was loaded with 10 µL of bromophenol blue tracking dye. The electrophoresis was performed under TBE buffer system for 50 min at constant voltage [20,21] of 50 V. Later the gel was allowed to rest for 0.5 h in 3 µL ethidium bromide solutions for staining purpose and also to avert hampering in intercalation. The gel was visualized using transilluminator.

Viscosity measurement: Hydrodynamic measurement is sensitive to the change in length (*i.e.*, viscosity) and it is considered as one of the reliable and most critical tests of the binding model in a solution. So viscosity studies were carried out to confirm the DNA binding mode. Viscosity of the solution increases when there is classical intercalation because during the process, lengthening of DNA helix occurs as the base pairs separates to accommodate the binding complex. In partial, non-classical intercalation the viscosity decreases due to bending or nicking of DNA helix, which further reduces its length. Above all no alteration in the viscosity of DNA solution is observed in case of groove or electrostatic binding. Whereas covalent binding leads to scission of DNA helix causes decrease in length and further decreases in the viscosity of the solution. A significant increase in the relative viscosity was observed upon addition of 8HQSPA metal chelates in DNA solution advocating intercalation binding nature of the compounds. The graph plot of $(\eta/\eta_0)^{1/3}$ *vs.* [DNA]/[complex] is represented in Fig. 6 gives a measure of the viscosity change [37].

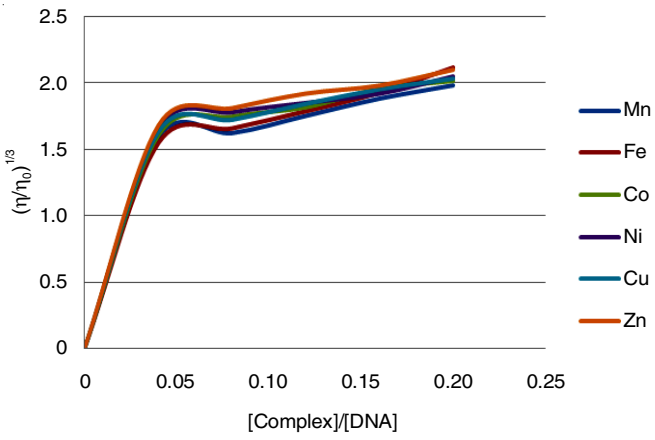

Fig. 6. Measurement of viscosity changes

Electronic absorption titration: Absorption titration by UV-Vis spectrophotometer was carried out to study the binding mode of metal chelates with CT-DNA strand. This is done by investigating the spectrum in the absence and presence of increasing concentration of DNA and a fixed concentration of 8HQMBS/metal chelates (10 µL). The observable hypochromism red shift is usually characterized by non-covalently intercalative binding of metal chelates to DNA helix, which is due to the strong stacking interaction between the aromatic chromophore of the metal chelates and DNA base pairs [38]. The UV-visible spectrum of CT DNA alone and on binding with metal chelates from a→g is represented in Fig. 7. From the spectrum it is clearly visible that the wavelength is shifted towards the right (red shift), which considered as intercalation binding mode.

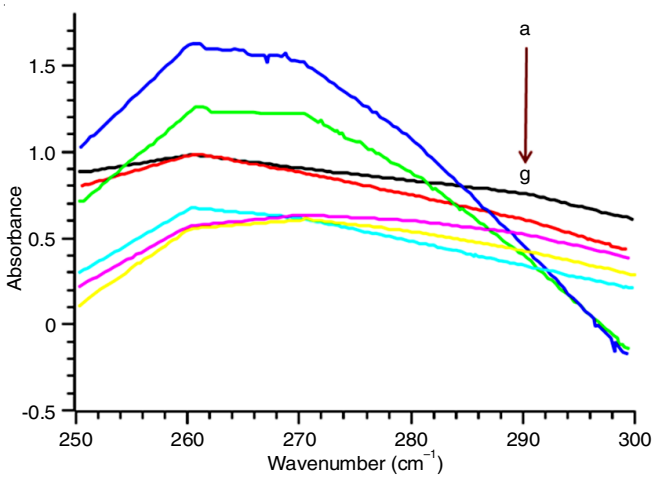

Fig. 7. UV-visible absorption titration spectra of 8HQSPA and its metal chelates with CT- DNA (a = CT DNA, b→g = Cu(II), Ni(II), Zn(II), Co(II), Fe(II) and Mn(II) chelates (50 µM) of CT-DNA (tris HCl buffer, pH 7.2)

Gel retardation assay by gel electrophoresis: The gel electrophoresis is a useful tool to investigate the mobility of DNA in the agarose gel environment on the influx of electric potential. In the present study, change in the electrophoretic mobility of calf thymus DNA (CT-DNA) in the absence and presence of chelates are considered as proof of complex DNA-interaction. The difference in the migration path length of complex-DNA than that of CT-DNA alone is usually considered as verification of complex-DNA interaction. Delayed in migration time of CT-DNA is due to the raise in the molecular weight, size and shape after interaction with complexes. The electro-phoretogram represented in Fig. 8, shows that the complex interaction retards the migration of CT-DNA, which visibly proves the complex-DNA intercalation [39].

Conclusion

A novel bidentate ligand (8HQSPA) was prepared in the molar ratio 1:1 of 5-amino-8-hydroxyquinoline and 4-acetamidobenzenesulfonyl chloride using pyridine as solvent and catalyst. The metal chelates was prepared in the molar ratio 2:1 of 8HQSPA and its metal(II) chloride in ethanol with good yield. The characterization of ligand 8HQSPA was done by ESI-MASS, FTIR, ^{1}H NMR, ^{13}C NMR and thermogravimetric analysis which proved the proposed structure have been synthesized. Metal chelates were characterized by various physico-chemical and elemental analysis, by FTIR and thermogravi-

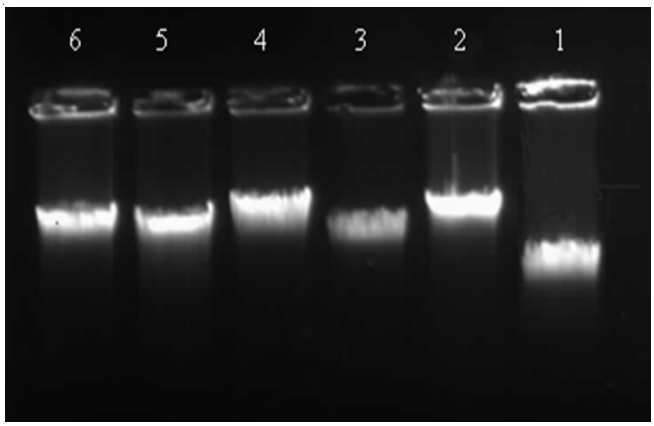

Fig. 8. Agarose gel electrophoresis image consist of CT-DNA = Lane 1, Lane 2-6 consists of DNA+Zn, DNA+Ni, DNA+Cu, DNA+Co and DNA+Fe complexes, respectively

metric analysis. Thermogravimetric analysis result showed the presence of two water molecules in the coordination, which gives the idea of octahedral geometrical arrangement of molecules. The electronic spectra showed transition of both ligand field and charge transfer bands, which confirms the synthesis of metal chelates. *in silico* ADMET result showed that the compounds are having good bioavailability on oral administration and are less toxic so they can be considered as a good drug candidate which further confirmed by *in vitro* analysis. Molecular docking studies was carried out on bacterial proteins (PDB ID: 5h67, 3ty7, 3t88 & 5i39) which showed minimum binding energy is required for the synthesized compounds to fit in the protein receptor pocket. Binding mode with DNA helix (PDB ID: 1BNA) was also studied and confirmed the intercalation mode. The antimicrobial activity tests were also done on two Gram-positive (*Staphylococus aureus* and *Bacillus subtilis*) and two Gram-negative (*Pseudomonas aeruginosa* and *Escherichia coli*) bacterial strains. Results showed that metal chelates of 8HQSPA are giving better activity than 8HQSPA ligand in the following increasing order: Cu > Fe > Zn > Ni > Co > Mn > 8HQSPA > sulphanalamide sulphate. This is due to increase in lipophilicity behaviour of 8HQSPA upon metal complexation and resulted geometrical arrangement. DNA binding studies were also carried out by various techniques like viscosity measurement, UV-visible spectroscopy, gel retardation assay by agarose gel electrophoresis. The result showed that 8HQSPA and its metal chelates binds through intercalation mode with DNA helix. This concludes that the synthesized compounds have promising applications, which may lead to design new and effective nucleic acid molecular probes and new therapeutic agents foe diseases on the molecular level.

ACKNOWLEDGEMENTS

Authors are thankful to Charutar Vidya Mandal, Vallabh Vidyanagar and Head, ARIBAS for providing research facility. One of the authors, Ruby Kharwar also gratefully acknowledges NFHE-ST (NFST-2015-17-ST-GUJ-1735) for providing financial support. The service of Director SICART, Vallabh Vidyanagar, for NMR and MASS analysis and PDPIAS, CHARUSAT for TGA analysis is gratefully acknowledge.

REFERENCES

1. R.E. Duval, M. Grare and B. Demoré, Fight Against Antimicrobial Resistance: We Always Need New Antibacterials but for Right Bacteria, *Molecules*, **24**, 3152 (2019); https://doi.org/10.3390/molecules24173152
2. S.R. Norrby, C.E. Nord and R. Finch, Lack of Development of New Antimicrobial Drugs: A Potential Serious Threat to Public Health, *Lancet Infect. Dis.*, **5**, 115 (2005); https://doi.org/10.1016/S1473-3099(05)01283-1
3. S.N. Al-Busafi, F.O. Suliman and Z.R. Al-Alawi, Synthesis, Characterization and Electronic Effects Investigations of New 5,7-disubstituted *tris*(8-quinolinolate)Al(III) Complexes, *Dyes Pigments*, **103**, 138 (2014); https://doi.org/10.1016/j.dyepig.2013.12.007
4. Y. Song, H. Xu, W. Chen, P. Zhan and X. Liu, 8-Hydroxyquinoline: A Privileged Structure with a Broad-ranging Pharmacological Potential, *MedChemComm*, **6**, 61 (2015); https://doi.org/10.1039/C4MD00284A
5. V. Prachayasittikul, V. Prachayasittikul, S. Prachayasittikul and S. Ruchirawat, 8-Hydroxyquinolines: A Review of their Metal Chelating Properties and Medicinal Applications, *Drug Des. Devel. Ther.*, **7**, 1157 (2013); https://doi.org/10.2147/DDDT.S49763
6. M. Kubanik, H. Holtkamp, T. Söhnel, S.M. Jamieson and C.G. Hartinger, Impact of the Halogen Substitution Pattern on the Biological Activity of Organoruthenium 8-Hydroxyquinoline Anticancer Agents, *Organometallics*, **34**, 5658 (2015); https://doi.org/10.1021/acs.organomet.5b00868
7. V.F.S. Pape, N.V. May, G.T. Gál, I. Szatmári, F. Szeri, F. Fülöp, G. Szakács and É.A. Enyedy, Impact of Copper and Iron Binding Properties on the Anticancer Activity of 8-Hydroxyquinoline Derived Mannich Bases, *Dalton Trans.*, **47**, 17032 (2018); https://doi.org/10.1039/C8DT03088J
8. S.F. Vanparia, T.S. Patel, R.B. Dixit and B.C. Dixit, Synthesis and *in vitro* Antimicrobial Activity of Some Newer Quinazolinone-Sulfonamide Linked Hybrid Heterocyclic Entities Derived from Glycine, *Med. Chem. Res.*, **22**, 5184 (2013); https://doi.org/10.1007/s00044-012-0320-7
9. V. Oliveri and G. Vecchio, 8-Hydroxyquinolines in Medicinal Chemistry: A Structural Perspective, *Eur. J. Med. Chem.*, **120**, 252 (2016); https://doi.org/10.1016/j.ejmech.2016.05.007
10. V. Algarsamy, Textbook of Medicinal Chemistry, Elsevier Health Sciences, vol. 11, p. 229 (2013).
11. R.B. Silverman and M.W. Holladay, The Organic Chemistry of Drug Design and Drug Action, Academic Press (2014).
12. S. Apaydin and M. Török, Sulfonamide Serivatives as Multi-Target Agents for Complex Diseases, *Bioorg. Med. Chem. Lett.*, **29**, 2042 (2019); https://doi.org/10.1016/j.bmcl.2019.06.041
13. U. Ndagi, N. Mhlongo and M.E. Soliman, Metal Complexes in Cancer Therapy-An Update from Drug Design Perspective, *Drug Des. Devel. Ther.*, **11**, 599 (2017); https://doi.org/10.2147/DDDT.S119488
14. N. Shahabadi, S. Kashanian and F. Darabi, DNA Binding and DNA Cleavage Studies of a Water Soluble Cobalt(II) Complex Containing Dinitrogen Schiff Base Ligand: The Effect of Metal on the Mode of Binding, *Eur. J. Med. Chem.*, **45**, 4239 (2010); https://doi.org/10.1016/j.ejmech.2010.06.020
15. J. Vora, S. Patel, S. Sinha, S. Sharma, A. Srivastava, M. Chhabria and N. Shrivastava, Structure Based Virtual Screening, 3D-QSAR, Molecular Dynamics and ADMET Studies for Selection of Natural Inhibitors Against Structural and Non-Structural Targets of Chikungunya, *J. Biomol. Struct. Dynam.*, **37**, 3150 (2018); https://doi.org/10.1080/07391102.2018
16. V. Thiyagarajan, K.W. Lee, M.K. Leong and C.F. Weng, Potential Natural mTOR Inhibitors Screened by *in silico* Approach and Suppress Hepatic Stellate Cells Activation, *J. Biomol. Struct. Dynam.*, **36**, 4220 (2018); https://doi.org/10.1080/07391102.2017.1411295
17. F. Shiri, S. Shahraki, S. Baneshi, M. Nejati-Yazdinejad and M.H. Majd, Synthesis, Characterization, *in vitro* Cytotoxicity, *in silico* ADMET Analysis and Interaction Studies of 5-Dithiocarbamato-1,3,4-thiadiazole-2-thiol and its Zinc(II) Complex with Human Serum Albumin: Combined Spectroscopy and Molecular Docking Investigations, *RSC Adv.*, **6**, 106516 (2016); https://doi.org/10.1039/C6RA17322E

18. R.B. Dixit, S.F. Vanparia, T.S. Patel, C.L. Jagani, H.V. Doshi and B.C. Dixit, Synthesis and Antimicrobial Activities of Sulfonohydrazide-substituted 8-Hydroxyquinoline Derivative and its Oxinates, *Appl. Organomet. Chem.*, **24**, 408 (2010); https://doi.org/10.1002/aoc.1631
19. J.A. Jacobsen, J.L. Fullagar, M.T. Miller and S.M. Cohen, Identifying Chelators for Metalloprotein Inhibitors Using a Fragment-Based Approach, *J. Med. Chem.*, **54**, 591 (2011); https://doi.org/10.1021/jm101266s
20. E.M. Kassem, E.R. El-Sawy, H.I. Abd-Alla, A.H. Mandour, D. Abdel-Mogeed and M.M. El-Safty, Synthesis of Certain New Fused Pyrano-pyrazole and Pyranoimidazole Incorporated into 8-Hydroxyquinoline through a Sulfonyl Bridge at Position 5 with Evaluation of their *in-vitro* Antimicrobial and Antiviral Activities, *Egyptian Pharm. J.*, **11**, 116 (2012); https://doi.org/10.7123/01.EPJ.0000421482.33940.0b
21. K. Singh, M.S. Barwa and P. Tyagi, Synthesis, Characterization and Biological Studies of Co(II), Ni(II), Cu(II) and Zn(II) Complexes with Bidentate Schiff Bases Derived by Heterocyclic Ketone, *Eur. J. Med. Chem.*, **41**, 147 (2006); https://doi.org/10.1016/j.ejmech.2005.06.006
22. S.S.S. Abuthahir, A.J.A. Nasser, S. Rajendran and G. Brindha, Synthesis, Spectral Studies and Antibacterial Activities of 8-Hydroxyquinoline Derivative and its Metal Complexes, *Chem. Sci. Transac.*, **3**, 303 (2014); https://doi.org/10.7598/cst2014.641
23. G.G. Mohamed and N.E. El-Gamel, Synthesis, Investigation and Spectroscopic Characterization of Piroxicam Ternary Complexes of Fe(II), Fe(III), Co(II), Ni(II), Cu(II) and Zn(II) with Glycine and dl-Phenylalanine, *Spectrochim. Acta A Mol. Biomol. Spectrosc.*, **60**, 3141 (2004); https://doi.org/10.1016/j.saa.2004.01.035
24. W. Wen, X. Yawen, J. Yin and Z. Wang, Gadolinium Complex of Schiff Base as Efficient Suppression Ratio for Hydroxyl Radical, *Asian J. Chem.*, **25**, 8307 (2013).
25. I.N. Witwit, Z.Y. Motaweq and H.M. Mubark, Synthesis, Characterization and Biological Efficacy on new mixed ligand Complexes Based from Azo Dye of 8-Hydroxyquinoline as a Primary Ligand and Imidazole as a Secondary Ligand with Some of Transition Metal Ions, *J. Pharm. Sci. Res.*, **10**, 3074 (2018).
26. Mudasir, N. Yoshioka and H. Inoue, DNA Binding of Iron(II) Mixed-Ligand Complexes Containing 1,10-Phenanthroline and 4,7-Diphenyl-1,10-phenanthroline, *J. Inorg. Biochem.*, **77**, 239 (1999); https://doi.org/10.1016/S0162-0134(99)00206-8
27. H.L. Jing, H.P. Zeng, Y.D. Zhou, T.T. Wang, G.Z. Yuan and X.H. Ouyang, Synthesis and Characterization of 8-Hydroxyquinoline Derivative Containing a Triphenylamine Unit and Its Metal Complexes, *Chin. J. Chem.*, **24**, 966 (2006); https://doi.org/10.1002/cjoc.200690183
28. R.M. Kirchner, C. Mealli, M. Bailey, N. Howe, L.P. Torre, L.J. Wilson, L.C. Andrews, N.J. Rose and E.C. Lingafelter, The Variable Coordination Chemistry of a Potentially Heptadentate Ligand with a Series of 3*d*-Transition Metal Ions. The Chemistry and Structures of $[M(py_3tren)]^{2+}$, where M(II) = Mn, Fe, Co, Ni, Cu and Zn and $(py_3tren) = N\{CH_2CH_2N{=}C(H)(C_5H_4N)\}_3$, *Coord. Chem. Rev.*, **77**, 89 (1987); https://doi.org/10.1016/0010-8545(87)85033-6
29. K.R. Seddon, ed.: A.B.P. Lever, Studies in Physical and Theoretical Chemistry; In: Inorganic Electronic Spectroscopy, Elsevier: Amsterdam, edn 2 (1985)
30. M. Sonmez and M. Sekerci, Synthesis and Characterization of Cu(II), Co(II), Ni(II) and Zn(II) Schiff Base Complexes from 1-Amino-5-benzoyl-4-phenyl-1*H*-pyrimidine-2-one with Salicylaldehyde, *Pol. J. Chem.*, **76**, 907 (2002).
31. A.V. Nikolaev, V.A. Logvinenko and L.L. Myachina, Thermal Analysis, Academic Press: New York (1969).
32. M. Gaber, N. El-Wakiel and O.M. Hemeda, Cr(III), Mn(II), Co(II), Ni(II) and Cu(II) Complexes of 7-((1*H*-Benzo[*d*]imidazol-2-yl)diazenyl)-5-nitroquinolin-8-ol. Synthesis, Thermal, Spectral, Electrical Measurements, Molecular Modeling and Biological Activity, *J. Mol. Struct.*, **1180**, 318 (2019); https://doi.org/10.1016/j.molstruc.2018.12.006
33. P. Jeyaraman, A. Alagarraj and R. Natarajan, *in silico* and *in vitro* Studies of Transition Metal Complexes Derived from Curcumin-Isoniazid Schiff Base, *J. Biomol. Struc. Dynam.*, **38**, 488 (2018); https://doi.org/10.1080/07391102.2019.1581090
34. E.M. Zayed, M.A. Zayed, A.M. Hindy and G.G. Mohamed, Coordination Behaviour and Biological Activity Studies Involving Theoretical Docking of *bis*-Schiff Base Ligand and Some of Its Transition Metal Complexes, *Appl. Organomet. Chem.*, **32**, 4603 (2018); https://doi.org/10.1002/aoc.4603
35. P. Arthi, S. Shobana, P. Srinivasan, L. Mitu and A.K. Rahiman, Synthesis, Characterization, Biological Evaluation and Docking Studies of Macrocyclic Binuclear Manganese(II) Complexes Containing 3,5-Dinitrobenzoyl Pendant Arms, *Spectrochim. Acta A Mol. Biomol. Spectrosc.*, **143**, 49 (2015); https://doi.org/10.1016/j.saa.2015.01.122
36. G. Eskici and P.H. Axelsen, Copper and Oxidative Stress in the Pathogenesis of Alzheimer′s Disease, *Biochemistry*, **51**, 6289 (2012); https://doi.org/10.1021/bi3006169
37. M.M.D. Anu, S.I. Pillai, C. Joel, R.B. Bennie, S. Subramanian and S.D. Kumar, Design, Synthesis, Characterization and DNA Interaction of New Schiff Base Metal Complexes, *J. Chem. Pharm. Res.*, **7**, 105 (2015).
38. S. Zehra, M.S. Khan, I. Ahmad and F. Arjmand, New Tailored Substituted Benzothiazole Schiff Base Cu(II)/Zn(II) Antitumor Drug Entities: Effect of Substituents on DNA Binding Profile, Antimicrobial and Cytotoxic Activity, *J. Biomol. Struct. Dynam.*, **37**, 1863 (2019); https://doi.org/10.1080/07391102.2018.1467794
39. T. Kondori, N. Akbarzadeh-T and C. Graiff, Synthesis, X-Ray Structural Analysis, Antibacterial and DNA-Binding Studies of a Lanthanum *bis*-(5,5′-Dimethyl-2,2′-bipyridine) Complex, *J. Iran. Chem. Soc*, **16**, 1827 (2019); https://doi.org/10.1007/s13738-019-01656-9